Journal of Power Sources 248 (2014) 679–684

Contents lists available at ScienceDirect

Journal of Power Sources

journal homepage: www.elsevier.com/locate/jpowsour

Influence of Li content on the structure and electrochemical performance of $Li_{1+x}Ni_{0.25}Mn_{0.75}O_{2.25+x/2}$ cathode for Li-ion battery

Yunjian Liu*, Yanyong Gao, Aichun Dou

School of Material Science and Technology, Jiangsu University, Zhenjiang, China

HIGHLIGHTS

- The cathode materials of $Li_{1+x}Ni_{0.25}Mn_{0.75}O_{2.25+x/2}$ ($x = 0$, 0.1, 0.2, 0.3, 0.4 and 0.5) have been synthesized.
- The layered-spinel composite structure is detected in the synthesized cathodes.
- The $Li_{1.3}Ni_{0.25}Mn_{0.75}O_{2.4}$ cathode shows the best electrochemical performance.

ARTICLE INFO

Article history:
Received 7 August 2013
Received in revised form
29 September 2013
Accepted 1 October 2013
Available online 11 October 2013

Keywords:
Lithium ion battery
Layered-spinel composited electrode
Lithium content
Electrochemical performance

ABSTRACT

The cathode materials of $Li_{1+x}Ni_{0.25}Mn_{0.75}O_{2.25+x/2}$ ($x = 0$, 0.1, 0.2, 0.3, 0.4 and 0.5) with different content of lithium have been synthesized in this paper. The materials with different lithium content show distinct differences in structure and charge/discharge characteristics. The layered-spinel composite structure has been detected in the $Li_{1+x}Ni_{0.25}Mn_{0.75}O_{2.25+x/2}$ electrodes, when the lithium content is lower than 1.5. The coulomb efficiency of $Li_{1+x}Ni_{0.25}Mn_{0.75}O_{2.25+x/2}$ electrode is increased with the content of lithium decreasing. The cyclic and rate performances of layered-spinel composite electrodes $Li_{1+x}Ni_{0.25}Mn_{0.75}O_{2.25+x/2}$ ($0 \le x \le 0.4$) are better than that of layered $Li_{1.5}Ni_{0.25}Mn_{0.75}O_{2.5}$. Among the layered-spinel composite electrodes, $Li_{1.3}Ni_{0.25}Mn_{0.75}O_{2.4}$ electrode shows the best capacity retention (98.2% for 40 cycles) and rate capacity (102 mAh g^{-1} at 10 C), while that of $Li_{1.5}Ni_{0.25}Mn_{0.75}O_{2.5}$ are 94.5% for 40 cycles and 11 mAh g^{-1} at 10 C. Electrochemical impedance spectroscopy (EIS) results show that the charge transfer resistance (R_{ct}) of $Li_{1.3}Ni_{0.25}Mn_{0.75}O_{2.4}$ electrode is lower than that of $Li_{1.5}Ni_{0.25}Mn_{0.75}O_{2.5}$. The enhanced cyclic and rate performances of $Li_{1.3}Ni_{0.25}Mn_{0.75}O_{2.4}$ cathode are attributed to the lower R_{ct}, three-dimensional interstitial space of $LiNi_{0.5}Mn_{1.5}O_4$ phase and the lower content of Li_2MnO_3 in $Li_{1.3}Ni_{0.25}Mn_{0.75}O_{2.4}$ cathode material.

1. Introduction

Recently, lithium rich layered oxides, which are solid solutions between layered Li_2MnO_3 and $LiMO_2$ (M = Ni, Co, Mn), have become attractive since they can exhibit high capacity of ~250 mAh g^{-1} when charged above 4.5 V [1–5]. Among these materials, $Li_{1.5}Ni_{0.25}Mn_{0.75}O_{2.5}$ delivers a high reversible capacity while being structurally stable upon charging to 4.6 V [3,5]. These properties, in addition to its being cobalt-free, make $Li_{1.5}Ni_{0.25}Mn_{0.75}O_{2.5}$ an excellent candidate to surmount the energy density shortfall of present lithium-ion batteries and to meet the lower cost and low toxicity requirement targeted by industry.

However, they exhibit inferior rate capability and lower coulombic efficiency in the first cycle. Surface modification has been reported to improve the rate capability and coulombic efficiency of the first cycle of lithium rich layered oxides [6–12]. Considering the complexity and limited improvement of surface modification, new method should be explored to improve the shortcomings of lithium rich layered oxides, including $Li_{1.5}Ni_{0.25}Mn_{0.75}O_{2.5}$ cathode material.

Among the discovered cathode materials, $LiNi_{0.5}Mn_{1.5}O_4$ has an operating voltage of ~4.7 V, and can be cycled between 2.0 and 4.9 V [13–15]. The $LiNi_{0.5}Mn_{1.5}O_4$ also exhibits high rate capability due to its three-dimensional diffusion of lithium ions. Fortunately, the Ni/Mn atom ratio of $LiNi_{0.5}Mn_{1.5}O_4$ is the same as $Li_{1.5}Ni_{0.25}Mn_{0.75}O_{2.5}$, and they can be synthesized using the same precursor ($Ni_{0.25}Mn_{0.75}CO_3$ or $Ni_{0.25}Mn_{0.75}(OH)_2$ [13]) and same method (solid-state method [14,16]). So Michael M. Thackeray [16,17], and K. Amine [18] have reported a new kind of cathode material

* Corresponding author. Tel.: +86 511 88790190.
E-mail address: lyjian122331@163.com (Y. Liu).

0378-7753/$ – see front matter © 2013 Elsevier B.V. All rights reserved.
http://dx.doi.org/10.1016/j.jpowsour.2013.10.006

composed of layered $Li_{1.5}Ni_{0.25}Mn_{0.75}O_{2.5}$ and spinel $LiNi_{0.5}Mn_{1.5}O_4$. In their reports, several kinds of the layered-spinel composite cathode materials have been presented. However, the electrochemical performance reported is not satisfied and the influences of lithium content on rate capability and first coulombic efficiency have not been studied in detail.

In this paper, the cathode materials of $Li_{1+x}Ni_{0.25}Mn_{0.75}O_{2.25+x/2}$ (x = 0, 0.1, 0.2, 0.3, 0.4, 0.5), which can also be written as $0.5yLiNi_{0.5}Mn_{1.5}O_4 \cdot (1-y)(Li_2MnO_3 \cdot LiNi_{0.5}Mn_{0.5}O_2)$ (y = 0.5, 0.4, 0.3, 0.2, 0.1, 0) correspondingly, have been synthesized by the co-precipitation method. The influences of lithium content on the structure and electrochemical performance of $Li_{1+x}Ni_{0.25}Mn_{0.75}O_{2.25+x/2}$ cathodes have been discussed in detail in this paper.

2. Experimental

The composite materials $Li_{1+x}Ni_{0.25}Mn_{0.75}O_{2.25+x/2}$ (x = 0, 0.1, 0.2, 0.3, 0.4, 0.5) were all synthesized by co-precipitation method as described below [15]. Required amounts of the transition metal acetates were dissolved in deionized water and then added drop by drop into a 0.1 M NaOH solution to form the co-precipitated hydroxides of Mn and Ni, which were then dried overnight at 120 °C in an air-oven, mixed with a required amount of lithium carbonate, heated in air at 500 °C for 4 h and 850 °C for 12 h, then quenched in liquid nitrogen.

X-ray diffraction (XRD) patterns of these samples were performed on a Panalytical X'Pert diffractometer (Holland) with Cu Kα radiation operated at 40 kV and 30 mA. Data were collected in 2θ range of 10–90° at 2° min^{-1}. Scanning electron microscopy (SEM) was performed on LEO1530 (Oxford Company). The Li content of layered-spinel electrode was tested by ICP-AES (Inductive Coupled Plasma-Atomic Emission Spectrometer).

Electrochemical measurements were carried out using R2025 coin-type cells. The positive electrodes were prepared by coating a mixture containing 80% active materials, 10% acetylene black, 10% poly (vinylidene fluoride) binder on circular Al current collector foils followed by drying at 120 °C for 1 h. The loading density of prepared electrode is 2.1 mg cm^{-2}. Electrochemical cells were assembled with the positive electrodes as-prepared, metallic lithium foil as counter electrode, Celgard 2400 as separator, and 1 M $LiPF_6$ dissolved in ethyl carbonate (EC) and dimethyl carbonate (DMC) (1:1 in volume) as electrolyte in an argon-filled glove box. Charge–discharge experiments were performed with 0.1 C (1 C = 240 mAh g^{-1}) between 2.0 and 4.8 V on battery testers (Land CT2001A).

The electrochemical impedance spectroscopy (EIS) of the cell, which was charged to 4.3 V, was measured using CHI660D (Chenghua Instrument Co. Ltd, Shanghai). The amplitude of the AC signal was 5 mV over the frequency range between 100 kHz and 0.01 Hz.

3. Results and discussion

The Li content of synthesized materials have been tested by ICP-AES, and the results have been listed in Table 1. As seen in Table 1, the Li content of the electrodes tested by ICP is consistent with our design $Li_{1+x}Ni_{0.25}Mn_{0.75}O_{2.25+x/2}$ (x = 0, 0.1, 0.2, 0.3, 0.4 and 0.5) materials.

Table 1
Li content of layered-spinel composite electrodes tested by ICP-AES.

Electrodes	Li content
$LiNi_{0.25}Mn_{0.75}O_{2.25}$	0.996
$Li_{1.1}Ni_{0.25}Mn_{0.75}O_{2.3}$	1.108
$Li_{1.2}Ni_{0.25}Mn_{0.75}O_{2.35}$	1.213
$Li_{1.3}Ni_{0.25}Mn_{0.75}O_{2.4}$	1.305
$Li_{1.4}Ni_{0.25}Mn_{0.75}O_{2.45}$	1.397
$Li_{1.5}Ni_{0.25}Mn_{0.75}O_{2.5}$	1.510

Fig. 1(a) compares the XRD patterns of $Li_{1+x}Ni_{0.25}Mn_{0.75}O_{2.25+x/2}$ electrodes. The selected segments (34–50°) of XRD patterns added with layered and spinel phase have been shown in Fig. 1(b). As shown, except of the layered $Li_{1.5}Ni_{0.25}Mn_{0.75}O_{2.5}$, all the other samples show both layered and spinel phase in the XRD patterns. Besides, the two superstructure reflections in the 2θ range of 20.5–22.5° appear more clearly with the lithium content increasing in the composite materials. The sharp superstructure reflections in the composite samples suggest a larger number of lithium ions in the transition metal layer than the expected based on the nominal composition [18,19]. So the degree of Li residing at transition metal layer of $Li_{1+x}Ni_{0.25}Mn_{0.75}O_{2.25+x/2}$ is increased with lithium content increasing.

The morphology of synthesized $Li_{1+x}Ni_{0.25}Mn_{0.75}O_{2.25+x/2}$ electrodes investigated by scanning electron microscopy is shown in Fig. 2. The SEM images in Fig. 2 show that the powders contain the aggregates of primary particles. The primary particles are homogenous and have a small size between 200 and 300 nm. The submicron size particles should result in better discharge capacity and rate performance [20].

To confirm the formation of layer-spinel composite structure, the micro-structure of the $Li_{1.3}Ni_{0.25}Mn_{0.75}O_{2.4}$ ($0.1LiNi_{0.5}Mn_{1.5}O_4 \cdot 0.8(Li_2MnO_3 \cdot LiNi_{0.5}Mn_{0.5}O_2)$) and $Li_{1.5}Ni_{0.25}Mn_{0.75}O_{2.5}$ ($Li_2MnO_3 \cdot LiNi_{0.5}Mn_{0.5}O_2$) particles investigated by high-resolution transmission electron microscope (HRTEM) technology are shown

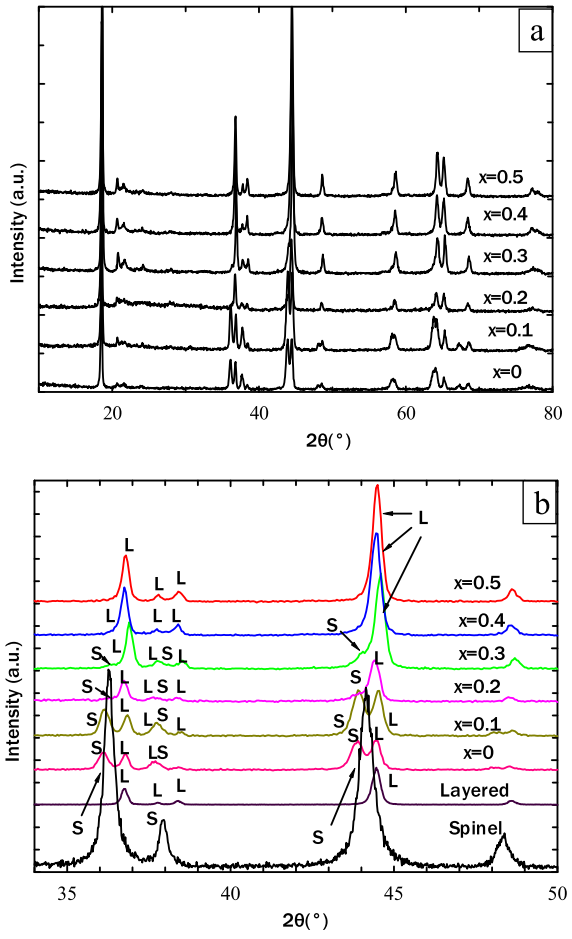

Fig. 1. XRD patterns of synthesized $Li_{1+x}Ni_{0.25}Mn_{0.75}O_{2.25+x/2}$.

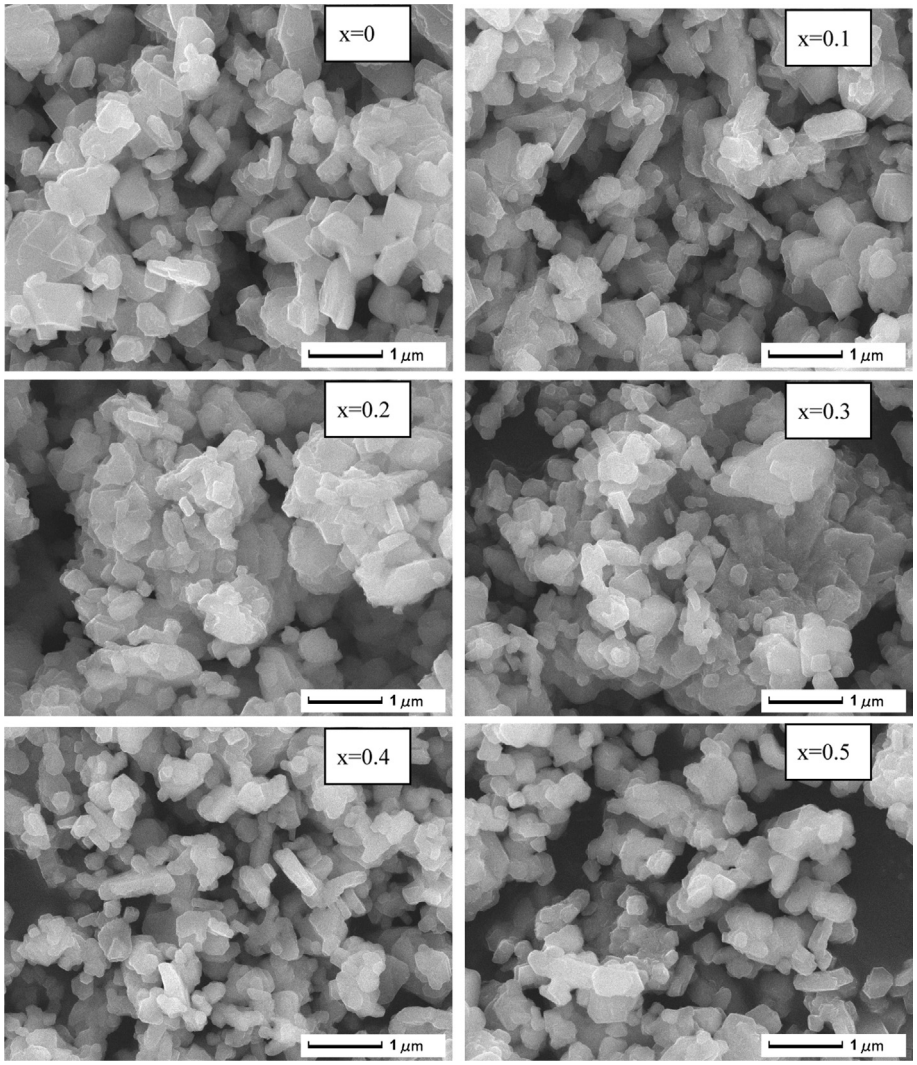

Fig. 2. Scanning electron microscopy (SEM) images of $Li_{1+x}Ni_{0.25}Mn_{0.75}O_{2.25+x/2}$.

in Fig. 3. The corresponding fast Fourier transform (FFT) images are also given in Fig. 3(1)–(3). As seen in Fig. 3(b) and (3), the layered structure of $Li_{1.5}Ni_{0.25}Mn_{0.75}O_{2.5}$ can be indexed clearly. Compared with Fig. 3(b) and (3), the HRTEM image in Fig. 3(a) combined with corresponding FFT images in Fig. 3(1) and (2) clearly show the composite character of product in which nano-sized domains of the layered (Fig. 3(1)) and spinel (Fig. 3(2)) components are structurally integrated. The result shows that the spinel and layered phases are integrated in the $Li_{1.3}Ni_{0.25}Mn_{0.75}O_{2.4}$ cathode effectively.

Fig. 4(a) shows the first charge/discharge curves of synthesized electrodes $Li_{1+x}Ni_{0.25}Mn_{0.75}O_{2.25+x/2}$ at 0.1 C between 2.0 and 4.8 V with constant current–constant voltage (CC–CV) method, and Fig. 4(b) shows the selected segment of charge/discharge curves. The charging process stops when the current decreases to 0.01 C. The $Li_{1+x}Ni_{0.25}Mn_{0.75}O_{2.25+x/2}$ electrodes can be fully charged with constant current–constant voltage (CC–CV) method. All the prepared samples have two distinguished voltage regions during the initial charge process. The appearance of a charge plateau at 4.5 V has been caused by the removal of Li_2O from the structure of Li_2MnO_3 [16]. There are plateaus at 4.8 V in the charge curves, which is the constant voltage plateau. As shown in Fig. 4, there are another three obvious plateaus at 4.7 (Figs. 4(b)), 2.8 and 2.2 V in the discharge curves of $LiNi_{0.25}Mn_{0.75}O_{2.25}$ ($0.25LiNi_{0.5}Mn_{1.5}O_4 \cdot 0.5(Li_2MnO_3 \cdot LiNi_{0.5}Mn_{0.5}O_2)$) and $Li_{1.1}Ni_{0.25}Mn_{0.75}O_{2.3}$ ($0.2LiNi_{0.5}Mn_{1.5}O_4 \cdot 0.6(Li_2MnO_3 \cdot LiNi_{0.5}Mn_{0.5}O_2)$). To our knowledge, the 4.7 V plateau originates from the Ni^{2+}/Ni^{4+} redox couple and the ordering of lithium at 8a sites with 50% filling in the $LiNi_{0.5}Mn_{1.5}O_4$ phase [20]. The other two reaction plateaus under 3.0 V (2.8 and 2.2 V) are associated with the reversible, first-order spinel Li$[Ni_{0.5}Mn_{1.5}]O_4$ to rocksalt $Li_2[Ni_{0.5}Mn_{1.5}]O_4$ transformation (2.8 V) [16] and then transformed to tetragonal ($I4_1/amd$) phase (2.2 V) at fully discharged state [21].

Table 2 compares the first charge and discharge capacities, ICL values and coulombic efficiencies of $Li_{1+x}Ni_{0.25}Mn_{0.75}O_{2.25+x/2}$ materials. As seen in Table 2, the discharge capacity of $Li_{1.3}Ni_{0.25}Mn_{0.75}O_{2.4}$ ($0.1LiNi_{0.5}Mn_{1.5}O_4 \cdot 0.8(Li_2MnO_3 \cdot LiNi_{0.5}Mn_{0.5}O_2)$) electrode is the highest, 282 mAh g^{-1}. Besides, the coulombic efficiency is increased with the decreasing content of lithium, and the coulombic efficiency of $LiNi_{0.25}Mn_{0.75}O_{2.25}$ ($0.25LiNi_{0.5}Mn_{1.5}O_4 \cdot 0.5(Li_2MnO_3 \cdot LiNi_{0.5}Mn_{0.5}O_2)$) is the highest, 88.2%. As reported [4], the irreversible capacity loss is due to the extraction of lithium as "Li_2O" on charging from Li_2MnO_3. The content of Li_2MnO_3 in the $Li_{1+x}Ni_{0.25}Mn_{0.75}O_{2.25+x/2}$ decreases with lower Li content, which results in lower irreversible capacity loss and higher coulombic efficiency. In our opinion, the discharge capacity under 3 V of $LiNi_{0.5}Mn_{1.5}O_4$ should be another reason for

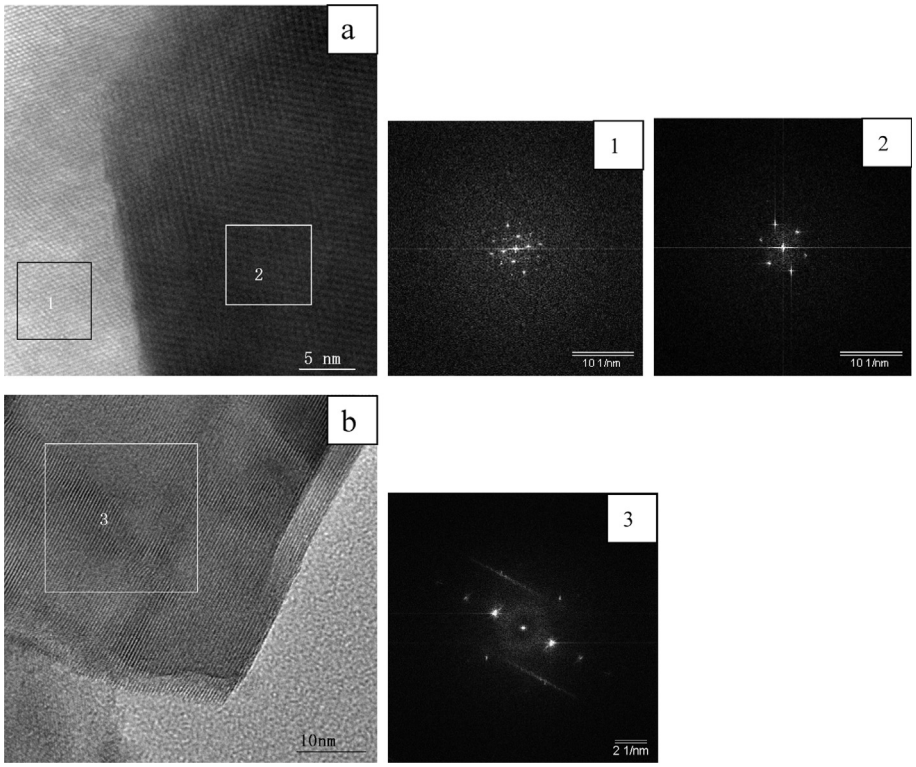

Fig. 3. TEM images with corresponding indexed fast Fourier transform (FFT) of the (a) $Li_{1.3}Ni_{0.25}Mn_{0.75}O_{2.4}$ and (b) $Li_{1.5}Ni_{0.25}Mn_{0.75}O_{2.5}$.

higher coulombic efficiency of layered-spinel composite electrodes in the first cycle.

Fig. 5 shows the differential capacity vs. voltage (dQ/dV) curves of $Li_{1.3}Ni_{0.25}Mn_{0.75}O_{2.4}$ ($0.1LiNi_{0.5}Mn_{1.5}O_4 \cdot 0.8(Li_2MnO_3 \cdot LiNi_{0.5}Mn_{0.5}O_2)$) and $Li_{1.5}Ni_{0.25}Mn_{0.75}O_{2.5}$ ($Li_2MnO_3 \cdot LiNi_{0.5}Mn_{0.5}O_2$) electrodes. The first charge curves exhibited two distinct oxidation peaks at around 3.8 and 4.6 V. The peak near 3.8 V is due to the oxidation of Ni^{2+} to Ni^{4+} [22]. The peak near 4.6 V is due to the irreversible removal of lithium and oxygen as Li_2O from Li_2MnO_3. The peaks observed below 3.5 V in the discharge curves are due to the Mn^{3+}/Mn^{4+} redox-reaction. As seen in Fig. 5, another peak positioned below 3.0 V in the discharge curve of $Li_{1.3}Ni_{0.25}Mn_{0.75}O_{2.4}$ electrode, which is associated with the reversible, first-order spinel $Li[Ni_{0.5}Mn_{1.5}]O_4$ to rock-salt $Li_2[Ni_{0.5}Mn_{1.5}]O_4$ transformation, is in agreement with discharge curves and XRD patterns.

Discharge capacity (0.2 C) versus cycle number plots for the first 40 cycles of the various lithium cells when cycled between 4.8 and 2 V are shown in Fig. 6. The discharge capacity retentions of $Li_{1+x}Ni_{0.25}Mn_{0.75}O_{2.25+x/2}$ ($x = 0$, 0.1, 0.2, 0.3, 0.4 and 0.5) are 96.1%, 97.8%, 97.9%, 98.2, 96.5% and 94.5%, respectively. The results show that the capacity retention of $Li_{1.5}Ni_{0.25}Mn_{0.75}O_{2.5}$ is lower than that of other layered-spinel composite materials, and the cyclic performance of $Li_{1.3}Ni_{0.25}Mn_{0.75}O_{2.4}$ ($0.1LiNi_{0.5}Mn_{1.5}O_4 \cdot 0.8(Li_2MnO_3 \cdot LiNi_{0.5}Mn_{0.5}O_2)$) is the best. As concluded in the Ref. [15], the existence of $LiNi_{0.5}Mn_{1.5}O_4$ spinel phase is beneficial for the cycle life performance of layered lithium and manganese enriched oxides.

In order to evaluate the lithium content on the rate capability of $Li_{1+x}Ni_{0.25}Mn_{0.75}O_{2.25+x/2}$ electrodes, the cells have been cycled in the voltage window from 2.0 to 4.8 V. Fig. 7 shows the discharge capacities of $Li_{1+x}Ni_{0.25}Mn_{0.75}O_{2.25+x/2}$/Li cells as a function of C-rate between 2.0 and 4.8 V. All of the cells have been charged at

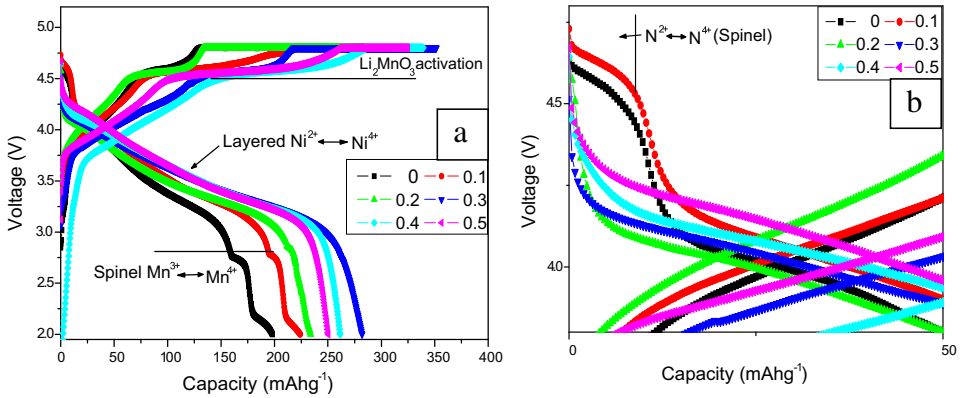

Fig. 4. First charge/discharge curves of $Li_{1+x}Ni_{0.25}Mn_{0.75}O_{2.25+x/2}$.

Table 2
Electrochemical cell data collected at 0.1 C rate and 2.0–4.8 V of the layered oxide cathodes.

Samples	Charge capacity mAh g^{-1}	Discharge capacity mAh g^{-1}	Irreversible capacity loss mAh g^{-1}	Coulomb efficiency %
1.0	224.6	198.1	26.5	88.2
1.1	260.3	224	36.3	86.1
1.2	284.2	233.9	50.3	82.3
1.3	351.3	282	69.3	80.2
1.4	339	261.4	77.6	77.1
1.5	336.7	250	86.7	74.3

0.1 C-rate, and then discharged at different C-rates from 0.1 to 10 C-rates. As the applied current density increases, all the samples show gradual decreases of discharge capacity. Among the tested samples, the layered-spinel composite electrodes show relatively moderate rate capacity fading compared with layered solid solution electrode $Li_{1.5}Ni_{0.25}Mn_{0.75}O_{2.5}$ ($Li_2MnO_3 \cdot LiNi_{0.5}Mn_{0.5}O_2$) as the applied current density increasing. And the $Li_{1.3}Ni_{0.25}Mn_{0.75}O_{2.4}$ ($0.1LiNi_{0.5}Mn_{1.5}O_4 \cdot 0.8(Li_2MnO_3 \cdot LiNi_{0.5}Mn_{0.5}O_2)$) electrode exhibits the best rate performance. The discharge capacity of $Li_{1.3}Ni_{0.25}Mn_{0.75}O_{2.4}$ electrode at 10 C is 102 mAh g^{-1}, while that of $Li_{1.5}Ni_{0.25}Mn_{0.75}O_{2.5}$ is only 11 mAh g^{-1}. The results show that the rate performance of layered solid solution is improved effectively by spinel phase doping.

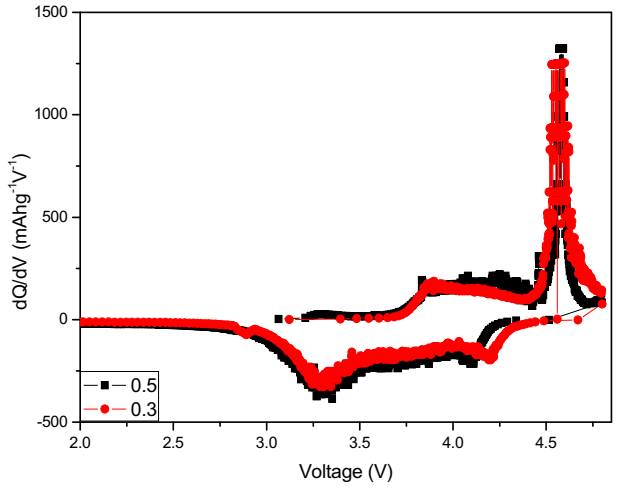

Fig. 5. Differential capacity vs. voltage (d*Q*/d*V*) curves of $Li_{1.3}Ni_{0.25}Mn_{0.75}O_{2.4}$ and $Li_{1.5}Ni_{0.25}Mn_{0.75}O_{2.5}$ electrodes.

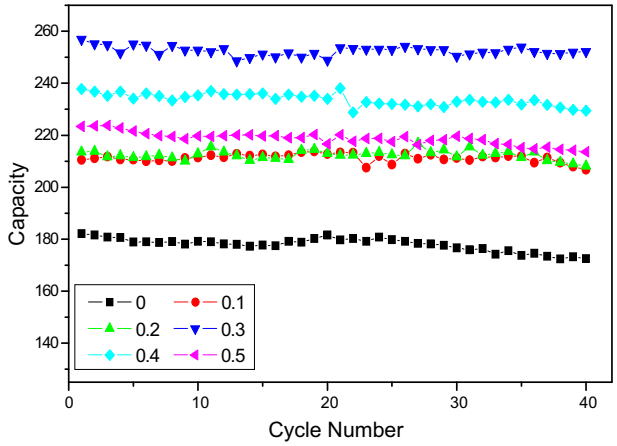

Fig. 6. Cyclic performance of $Li_{1+x}Ni_{0.25}Mn_{0.75}O_{2.25+x/2}$ electrodes.

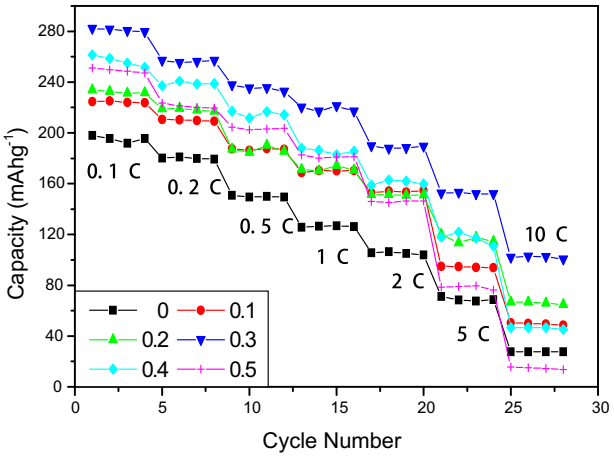

Fig. 7. Discharge capacity as a function of C rate for $Li_{1+x}Ni_{0.25}Mn_{0.75}O_{2.25+x/2}$.

As reported in Ref. [23], one of the plausible causes for the poor rate capability of $Li_{1.5}Ni_{0.25}Mn_{0.75}O_{2.5}$ ($Li_2MnO_3 \cdot LiNi_{0.5}Mn_{0.5}O_2$) at high-current density may be related to high polarization due to partially blocked Li diffusion pathway. It has been reported by Croguennec [24] that the high polarization in $Li[Li_{0.12}Ni_{0.425}Co_{0.15}Mn_{0.425}]O_2$ is usually observed after oxygen loss in the first cycle which caused the movement of Ni into the Li layer during oxygen loss and partial blocking of Li diffusion pathway. Besides, the phenomena that the spinel component can provide the electrode with a high-rate capability have been reported [24,25]. Compare with layered-spinel composite materials $Li_{1+x}Ni_{0.25}Mn_{0.75}O_{2.25+x/2}$ ($0 \le x \le 0.4$) ($0.5yLiNi_{0.5}Mn_{1.5}O_4 \cdot (1-y)$ ($Li_2MnO_3 \cdot LiNi_{0.5}Mn_{0.5}O_2$) ($0.5 \le y \le 0.1$)), $Li_{1.5}Ni_{0.25}Mn_{0.75}O_{2.5}$ ($Li_2MnO_3 \cdot LiNi_{0.5}Mn_{0.5}O_2$) contains a higher amount of Li_2MnO_3 and absence of $LiNi_{0.5}Mn_{1.5}O_4$ in the structure. Thus the relatively large amount of irreversible loss of oxygen in the first cycle and the poor rate capability of $Li_{1.5}Ni_{0.25}Mn_{0.75}O_{2.5}$ could be expected.

Electrochemical impedance spectroscopy (EIS) has been performed to get insights into the difference in electrochemical

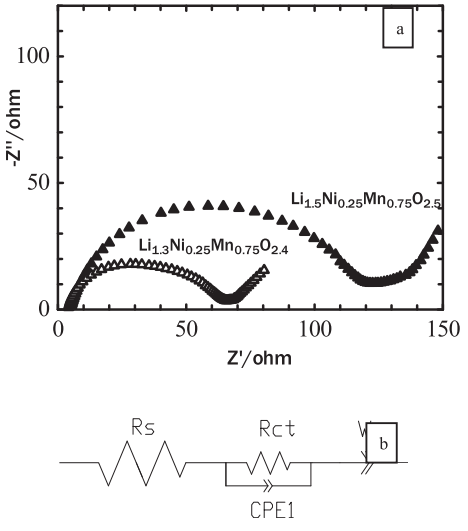

Fig. 8. AC impedance of $Li_{1.3}Ni_{0.25}Mn_{0.75}O_{2.4}$ and $Li_{1.5}Ni_{0.25}Mn_{0.75}O_{2.5}$ electrodes (a) and equivalent circuit (b).

Table 3
Impedance parameters of equipment circuit.

Electrodes	R_s (Ω)	R_{ct} (Ω)
$Li_{1.3}Ni_{0.25}Mn_{0.75}O_{2.4}$	4.1	60.3
$Li_{1.5}Ni_{0.25}Mn_{0.75}O_{2.5}$	5.0	115.7

performance of $Li_{1.3}Ni_{0.25}Mn_{0.75}O_{2.4}$ ($0.1LiNi_{0.5}Mn_{1.5}O_4 \cdot 0.8(Li_2MnO_3 \cdot LiNi_{0.5}Mn_{0.5}O_2)$) and $Li_{1.5}Ni_{0.25}Mn_{0.75}O_{2.5}$ ($Li_2MnO_3 \cdot LiNi_{0.5}Mn_{0.5}O_2$). The measurements are carried out in the charged state of 4.4 V after 40 cycles tested at 0.1 C. The measured impedance spectra are presented in Fig. 8(a). A high-frequency semicircle and a low-frequency tail are observed. Generally, an intercept at the Z_{real}-axis in high frequency region corresponded to ohmic resistance (R_s). The high-frequency semicircle is related to charge transfer resistance (R_{ct}). The low-frequency tail is associated with Li^+ ion diffusion process in the solid phase of electrode. Each impedance spectrum is fitted with suggested equivalent circuit model (Fig. 8(b)) to give simulation of the ohmic resistance (R_s) and charge transfer resistance (R_{ct}), as summarized in Table 3. As seen in Table 3, the R_{ct} of $Li_{1.3}Ni_{0.25}Mn_{0.75}O_{2.4}$ is lower than that of $Li_{1.5}Ni_{0.25}Mn_{0.75}O_{2.5}$, indicating an enhancement in the kinetics of lithium-ion diffusion through surface layer and charge transfer reaction and a consequent increase in rate performance. The lower R_{ct} of $Li_{1.3}Ni_{0.25}Mn_{0.75}O_{2.4}$ is due to the three-dimensional interstitial space of $LiNi_{0.5}Mn_{1.5}O_4$ phase. Besides, the lower content of Li_2MnO_3 in the $Li_{1.3}Ni_{0.25}Mn_{0.75}O_{2.4}$, which causes lower content of oxygen release and less surface reaction with electrolyte, should result in thinner solid electrolyte interface (SEI) film and lower charge transfer reaction resistance.

4. Conclusion

The cathode materials $Li_{1+x}Ni_{0.25}Mn_{0.75}O_{2.25+x/2}$ ($x = 0$, 0.1, 0.2, 0.3, 0.4 and 0.5) which can also be translated to $0.5yLiNi_{0.5}Mn_{1.5}O_4 \cdot (1-y)(Li_2MnO_3 \cdot LiNi_{0.5}Mn_{0.5}O_2)$ ($y = 0.5$, 0.4, 0.3, 0.2, 0.1, 0) correspondingly, with different lithium content have been synthesized in this paper. Layered-spinel composite structure has been detected in the $Li_{1+x}Ni_{0.25}Mn_{0.75}O_{2.25+x/2}$ ($0 \le x \le 0.4$) materials, except of layered $Li_{1.5}Ni_{0.25}Mn_{0.75}O_{2.5}$ cathode. The coulombic efficiency of $Li_{1+x}Ni_{0.25}Mn_{0.75}O_{2.25+x/2}$ cathodes in the first cycle is increased with decreasing lithium content, and that of $LiNi_{0.25}Mn_{0.75}O_{2.25}$ is the highest (88.2%). The cyclic and rate performances of layered-spinel composite cathodes $Li_{1+x}Ni_{0.25}Mn_{0.75}O_{2.25+x/2}$ are better than that of layered $Li_{1.5}Ni_{0.25}Mn_{0.75}O_{2.5}$, and the $Li_{1.3}Ni_{0.25}Mn_{0.75}O_{2.4}$ cathode shows the best electrochemical performance. The discharge capacity of $Li_{1.3}Ni_{0.25}Mn_{0.75}O_{2.4}$ is 282 mAh g^{-1} at 0.1 C and 102 mAh g^{-1} at 10 C, and the capacity retention of $Li_{1.3}Ni_{0.25}Mn_{0.75}O_{2.4}$ is 98.2% after 40 cycles. The three-dimensional interstitial space of $LiNi_{0.5}Mn_{1.5}O_4$ phase, lower content of Li_2MnO_3 and lower charge transfer reaction resistance should be responsible for better electrochemical performance of $Li_{1.3}Ni_{0.25}Mn_{0.75}O_{2.4}$ electrode. This paper suggests that layered-spinel composite cathode $Li_{1.3}Ni_{0.25}Mn_{0.75}O_{2.4}$ could be a potential candidate material for the application of rechargeable Li-ion batteries in PHEVs.

Acknowledgement

The authors gratefully acknowledge the National Natural Science Foundation of China (51304081) and Postdoctoral Foundation of China (2012M511211).

References

[1] D.H. Kim, S.H. Kang, M. Balasubramanian, C.S. Johnson, Electrochem. Commun. 12 (2010) 1618–1621.
[2] F. Wu, H.Q. Lu, Y.F. Su, N. Li, L.Y. Bao, S. Chen, J. Appl. Electrochem 40 (2010) 783–789.
[3] J.G. Wen, J. Bareno, C.H. Lei, S.H. Kang, M. Balasubramanian, I. Petrov, D.P. Abraham, Solid State Ionics 182 (2011) 98–107.
[4] A.R. Armstrong, M. Holzapfel, P. Novak, C.S. Johnson, S.H. Kang, M.M. Thackeray, P.G. Bruce, J. Am. Chem. Soc. 128 (2006) 8694–8698.
[5] T. Ohzuku, M. Nagayama, K. Tsuji, K. Ariyoshi, J. Mater. Chem. 21 (2011) 10179–10188.
[6] Y.J. Liu, J. Lv, S.B. Liu, L. Chen, X.H. Chen, Powder Technol. 239 (2013) 461–466.
[7] J.M. Zheng, Z.R. Zhang, X.B. Wu, Z.X. Dong, Z. Zhu, Y. Yang, J. Electrochem. Soc. 155 (2008) A775–A782.
[8] Y. Wu, A. Manthiram, Electrochem. Solid State Lett. 9 (2006) A221–A224.
[9] Y. Wu, A. Manthiram, Solid State Ionics 180 (2009) 50–56.
[10] Y.J. Kang, J.H. Kim, S.W. Lee, Y.K. Sun, Electrochem. Acta 50 (2005) 4784–4791.
[11] J.M. Zheng, J. Li, Z.R. Zhang, X.J. Guo, Y. Yang, Solid State Ionics 179 (2008) 1794–1799.
[12] Y.J. Liu, S.B. Liu, Y.P. Wang, L. Chen, X.H. Chen, J. Power Sources 222 (2013) 455–460.
[13] J. Mao, K.H. Dai, Y.H. Zhai, Electrochim. Acta 63 (2012) 381–390.
[14] D.W. Shin, A. Manthiram, Electrochem. Commun. 13 (2011) 1213–1216.
[15] Y.J. Liu, L. Chen, Ionics 18 (2012) 649–653.
[16] S.H. Park, S.H. Kang, C.S. Johnson, K. Amine, M.M. Thackeray, Electrochem. Commun. 9 (2007) 262–268.
[17] J. Cabana, S.H. Kang, C.S. Johnson, M.M. Thackeray, C.P. Greya, J. Electrochem. Soc. 156 (2009) A730–A736.
[18] H.X. Deng, I. Belharouak, Y.K. Sunb, K. Amine, J. Mater. Chem. 19 (2009) 4510–4516.
[19] C.R. Fell, K.J. Carroll, M. Chi, Y.S. Meng, J. Electrochem. Soc. 157 (2010) A1202–A1207.
[20] J.C. Arrebola, A. Caballero, L. Hernan, J. Morales, J. Power Sources 180 (2008) 852–855.
[21] S.H. Park, S.W. Oh, S.H. Kang, I. Belharouak, K. Amine, Y.K. Sun, Electrochim. Acta 52 (2007) 7226–7230.
[22] N. Yabuuchi, Y. Makimura, T. Ohzuku, J. Electrochem. Soc. 154 (2007) A314–A318.
[23] J.H. Lim, H. Bang, K.S. Lee, K. Amine, J. Power Sources 189 (2009) 571–575.
[24] C.S. Johnson, N. Li, J.T. Vaughey, S.A. Hackney, M.M. Thackeray, Electrochem. Commun. 7 (2005) 528–530.
[25] B.H. Song, Z.W. Liu, M.O. Lai, L. Lu, Phys. Chem. Chem. Phys. 14 (2012) 12875–12883.